# Towards a Microfabricated Flexible Graphene-Based Active Implant for Tissue Monitoring During Optogenetic Spinal Cord Stimulation

Velea, Andrada Iulia; Vollebregt, S.; Hosman, T.B.; Pak, A.; Giagka, Vasiliki

**DOI**
10.1109/NMDC47361.2019.9084021

**Publication date**
2020

**Document Version**
Final published version

**Published in**
2019 IEEE 14th Nanotechnology Materials and Devices Conference, NMDC 2019

# Towards a Microfabricated Flexible Graphene-Based Active Implant for Tissue Monitoring During Optogenetic Spinal Cord Stimulation

Andrada Iulia Velea[1,2], Sten Vollebregt[2], Tim Hosman[1,3], Anna Pak[1,3], Vasiliki Giagka[1,3]

[1]*Bioelectronics Section and* [2]*Electronic Components, Technology and Materials Section, Department of Microelectronics, Delft University of Technology, Mekelweg 4, 2628 CD, Delft, The Netherlands*
[3]*Technologies for Bioelectronics Group, Department of System Integration and Interconnection Technologies, Fraunhofer Institute for Reliability and Microintegration IZM, Berlin, Germany*

A.I.Velea@student.tudelft.nl, S.Vollebregt@tudelft.nl, timothy.benjamin.hosman@izm.fraunhofer.de, A.Pak@tudelft.nl, V.Giagka@tudelft.nl

***Abstract* – This work aims to develop a smart neural interface with transparent electrodes to allow for electrical monitoring of the site of interest during optogenetic stimulation of the spinal cord. In this paper, a microfabrication process for the wafer-level development of such a compact, active, transparent and flexible implant is presented. Graphene has been employed to form the transparent array of electrodes and tracks, on top of which chips have been bonded using flip-chip bonding techniques. To provide high flexibility, soft encapsulation, using polydimethylsiloxane (PDMS) has been used. Making use of the "Flex-to-Rigid" (F2R) technique, cm-size graphene-on-PDMS structures have been suspended and characterized using Raman spectroscopy to qualitatively evaluate the graphene layer, together with 2-point measurements to ensure the conductivity of the structure. In parallel, flip-chip bonding processes of chips on graphene structures were employed and the 2-point electrical measurement results have shown resistance values in the range of kΩ for the combined tracks and ball-bonds.**

***Keywords* – Neural interface, optogenetic stimulation, transparent active implant, graphene, PDMS.**

## I. Introduction

Epidural spinal cord stimulation (ESCS) has been proven to promote locomotion recovery in patients affected by spinal cord injuries (SCIs) [1]. However, optimization of the specifications for such therapies is still under research and identifying the mechanism of action could greatly benefit from parallel monitoring of the response of the biological tissue during stimulation. Traditionally, in ESCS, energy is injected into the tissue in the form of electrical pulses, leading to activation. Recently, the use of light for activating the biological tissue after genetic modification of the cells, a method known as optogenetics, has been gaining popularity in the field of spinal cord stimulation, due to the fact that it enables more selective activation of the neural cells [2].

Most electrode arrays for ESCS feature opaque electrodes which limit the electrical monitoring of the tissue response during optogenetic excitation [3, 4]. Therefore there is the need to develop optically transparent, conductive, and flexible neural interfaces that can enable capturing the electrical activity of the neurons below the activation site at the time of stimulation. One potential material for these electrodes is graphene, as the material is optically transparent, bendable, potentially biocompatible, and has excellent electrical properties [5, 6]. Graphene microelectrode arrays have been previously reported as passive implants with Au tracks to interface the electrodes with the outside active system [5]. However, for a smart implant, ultimately, active components, e.g. integrated circuits (ICs), have to be embedded with the electrodes to allow for signal acquisition, in-situ amplification and processing.

The aim of the current work is the development, by means of microfabrication, of a compact, flexible, graphene-based, active spinal cord monitoring implant to be used during optogenetic stimulation.

## II. Materials and Methods

A microfabrication process has been used to ensure reproducibility and maintain the small size of the implant while achieving high resolution. Fig. 1 illustrates the process steps of the current work.

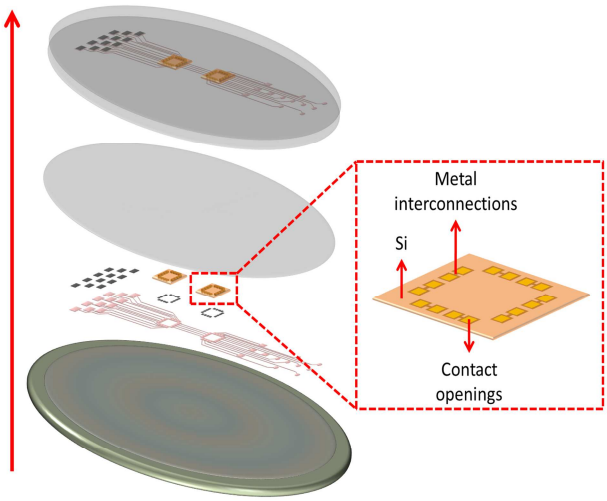


Fig. 1. Process steps of the proposed method. A molybdenum catalyst layer is used for graphene growth, on top of which chips are bonded and later, the complete structure is encapsulated in polymer.

978-1-7281-2637-1/19/$31.00 ©2019 IEEE

Chemical vapour deposited (CVD) graphene tracks and electrodes have been microfabricated on a silicon (Si) wafer, using a pre-patterned 50 nm molybdenum (Mo) layer as a catalyst, deposited on a silicon dioxide ($SiO_2$) layer as described in detail by Vollebregt et al., [7]. On top, metal was deposited and patterned to create a bonding interface between graphene and the gold (Au) stud bumps existent on the pads of the chips. Two different metallization versions were created; one consisted of 675 nm of aluminium (Al) and the other of 100 nm of titanium (Ti) and 675 nm of Al.

Chips were then bonded to the substrate using a thermocompression flip-chip bonding technique. As an underfill material and to improve the bonding stability, either an anisotropic conductive adhesive (ACA) (Toshiba TAP0212E) or a non-conductive adhesive (NCA) (Epotek 303-2FL) was manually applied to the substrate before bonding. The adhesive was pre-heated at 90 °C for 30 seconds for degassing purposes. Finally, the chips were bonded using a thermocompression bonding cycle of 60 seconds at 250 °C while applying roughly 19 MPa of pressure. The applied temperature also cured the adhesive. Next, 50 µm of Sylgard 184 polydimethylsiloxane (PDMS), 1:10 ratio, was spin-coated on top of the structure and cured at 90 °C for 1 hour. At this point, the complete structure had to be transferred or released from the original wafer in order to spin coat the final backside PDMS encapsulation layer. To do so, two approaches were investigated, as illustrated in Fig. 2.

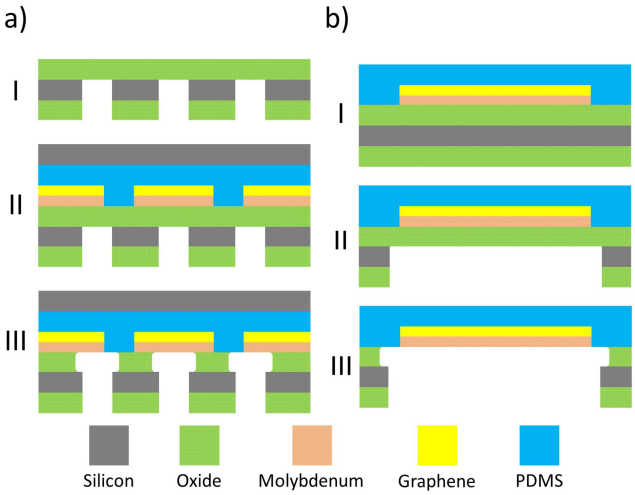


Fig. 2. Approaches used to transfer/ release the structure. In (a), a wet transfer approach, using buffered hydrofluoric acid (BHF) 7:1 for oxide etching. In (b), a "Flex-to-Rigid" (F2R) approach [8].

The approach in Fig. 2(a) consists of the creation of through-silicon vias (TSV), using a deep reactive ion etching (DRIE) process before graphene growth, to increase the number of access points for the etchant. The alternative approach in Fig. 2(b) consists of a DRIE process for cm-size suspended areas (that can later be coated with PDMS as final encapsulation), performed after the graphene growth completion, an approach known as Flex-to-Rigid (F2R) [8]. Any of the two aforementioned approaches is followed by a BHF 7:1 wet etching step for the removal of the remaining oxide layer which acts as a stopping layer for the DRIE process.

## III. Results and Discussion

### A. *Wafer-level graphene growth*

First, Raman spectroscopy was performed to ensure the presence of graphene after growth on the full wafer and to evaluate the quality of the layer at this step (Fig. 3).

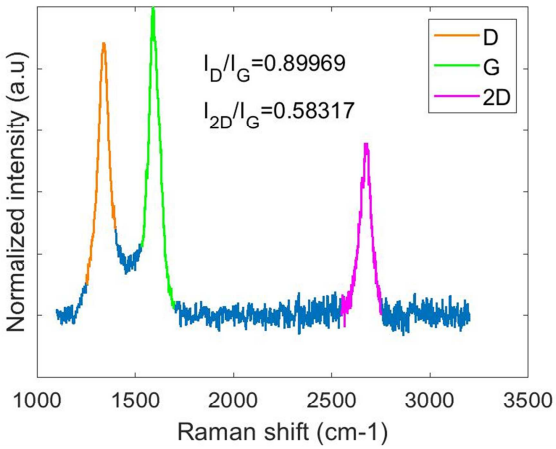


Fig. 3. Raman spectroscopy measurement, acquired using a 633 nm laser. The 3 peaks indicate the presence of graphene after the growth step.

Based on what has been previously reported in the literature, if graphene is present, the D band should appear at ~1330 $cm^{-1}$, G band at ~1590 $cm^{-1}$ and 2D band at ~2660 $cm^{-1}$ [9]. The ratio $I_{2D}/I_G$, greater than 1 for a monolayer graphene, suggests that multilayer graphene has been grown, since its value decreases significantly with the increase in number of layers [10]. This constitutes an advantage for this application due to the fact that within a multilayer graphene structure the grain boundaries will not be aligned, thus providing more mechanical stability, an important aspect for flexible devices. The ratio $I_D/I_G$ estimates the number of defects, originating from the growth process, present in the graphene layer (the greater the ratio, the more defects can be found) [7]. Ideally, if no defects are present, $I_D$ should be equal to 0 but as observed in Fig. 3, the D peak is relatively pronounced.

Besides Raman spectroscopy, 2-point measurements were conducted over an area of 70 µm in width and approximately 1 mm in length, to electrically evaluate the graphene tracks. The results can be observed in Fig. 4.

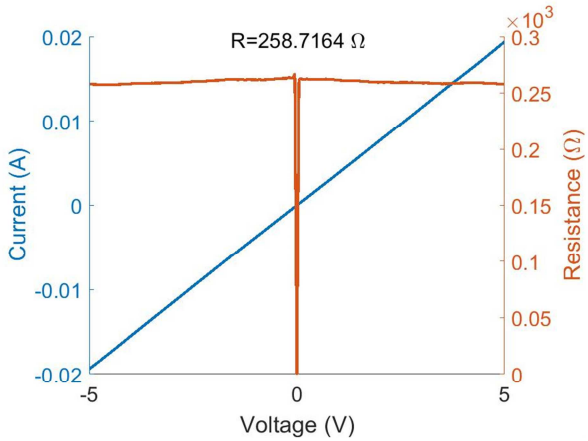


Fig. 4. 2-point measurement result over a graphene area of 70 um in width and 1 mm in length.

The measured resistance is ~250 Ω for a parallel configuration of Mo and graphene since, at this point, Mo has not been removed from the wafer.

### *B. "Wet" transfer of structure*

BHF etching of the oxide layer from beneath the structure has been tested. The expected etch rate was 150 nm/min and the total calculated etching time was 40 min. Yet, after 7 hours, no etching around the TSV has been observed. Possibly, DRIE of the TSV resulted in the deposition of a polymer layer which could not be removed by $O_2$-plasma treatment. To circumvent this, potassium hydroxide (KOH) etching was performed to widen the pathways for the BHF. However, after these long wet etching steps, the structures were highly damaged or even removed, likely due to the PDMS being affected by the etchants. Since later in the process, at this step, chips containing active components will also be present, wet transfer of the structure is to be avoided.

### *C. "Flex-to-rigid" approach*

Fig. 5 shows the structure after the F2R and oxide removal steps. The complete area of the implant, with Mo tracks and electrodes, was successfully suspended and the membranes did not contain any significant wrinkles or damages.

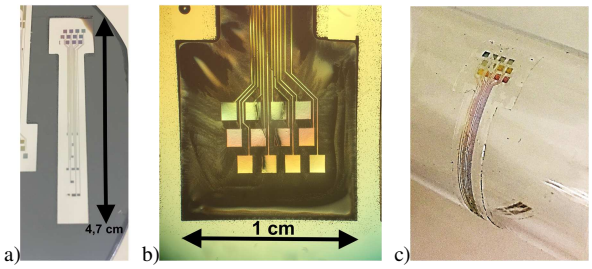


Fig. 5. Implant structure with Mo tracks after DRIE. In a), the complete suspended implant can be observed. In b), a detailed perspective of the PDMS membrane and tracks is presented. In c), the high flexibility of the structure is shown.

Fig. 6 illustrates the graphene-on-PDMS implant structures after the complete removal of the Mo layer using peroxide for ~ 5 min.

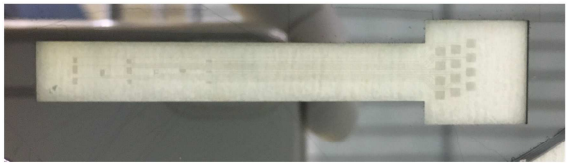

Fig. 6. Implant structure with graphene-only tracks and electrodes after F2R approach and catalyst removal. In this image the implant has not yet been released from the Si carrier wafer.

After the successful suspension of the graphene-on-PDMS structures, Raman spectroscopy evaluation has been conducted in order to ensure that the layer encapsulated in PDMS is graphene only. These results can be seen in Fig. 7.

The ratio $I_D/I_G$, which indicates the amount of defects present in the graphene layer, remains similar to the one measured after graphene growth and before any post-processing method has been applied. This result indicated that the transferring processes did not influence the quality of graphene. The ratio $I_{2D}/I_G$, which estimates the number of graphene layers present on the structure, increased compared to the previous measurements. The change in the measured value is likely influenced by the layer of material present underneath graphene, in this case PDMS, or previously, Mo on top of oxide [11]. The gray area represents the influence of PDMS over the measurement.

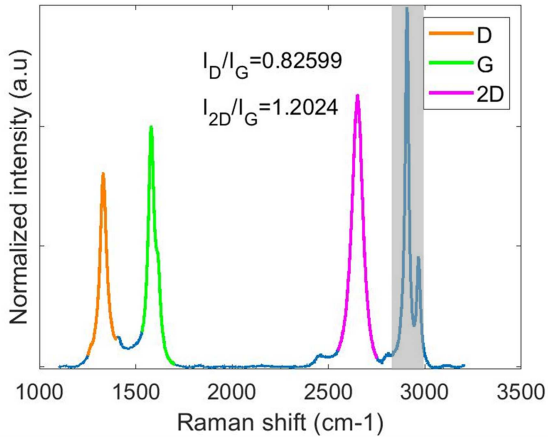


Fig. 7. Raman spectroscopy results after the suspension of the graphene-on-PDMS membranes.

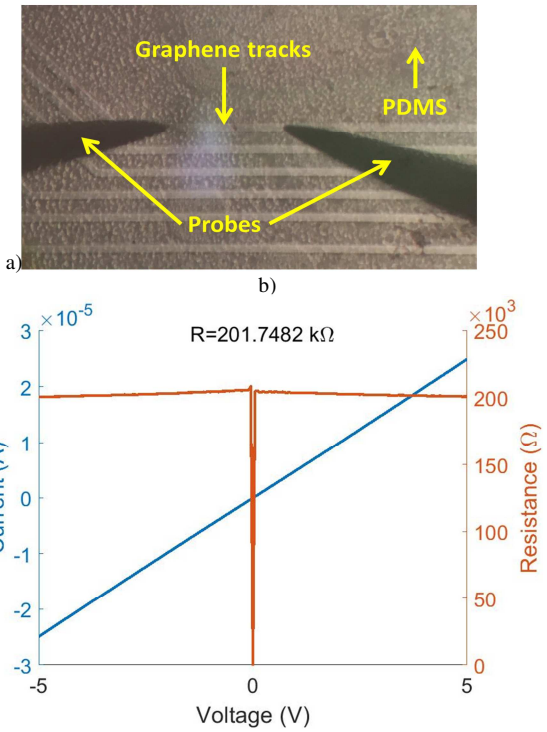


Fig. 8. 2-point measurement after releasing the structures using DRIE and wet etching steps for oxide and Mo removal. In a), the measurement points are illustrated. In b), the results obtained after the measurement can be observed.

A 2-point measurement evaluation has been conducted over the graphene tracks in order to evaluate their conductivity after Mo removal. Fig. 8 illustrates both measurement points as well as the I/(R)-V curves. The measured resistance value, for approximately the same area

of 70 µm in width and 1 mm in length, was in the range of kΩ (~200 kΩ), meaning that the resistance of Mo is much lower (cf. Fig. 4), thus having a great influence on the total resistance value when still underneath graphene.

An approximately square graphene pad (1050 µm by 910 µm) for which the dimensions do not influence the resistivity that much, therefore the resistivity resembles the sheet resistance of the material, showed a resistance value of about 7.5 kΩ as illustrated in Fig. 9.

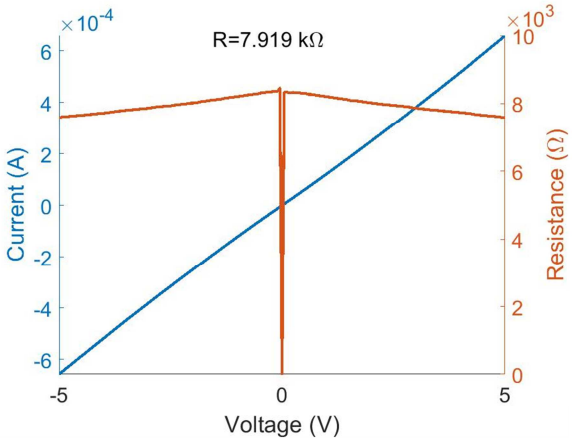


Fig. 9. 2-point measurement for a graphene pad of 1050 µm by 910 µmafter the release of the structures.

The influence of the contact resistance between graphene and the measurement probes, which is difficult to estimate, could play an important role in the measured value.

### *D. Flip-chip bonding*

So far, no flip-chip bonding processes on graphene substrates have been reported in the literature and our initial attempt on flip-chip bonding dummy chips directly on graphene showed that the adhesion between graphene and Au stud bumps is poor, therefore chips could not be bonded. Even when using an NCA, as a different flip-chip bonding technique, as presented in section II "Materials and Methods" of this paper, the 2-point measurement results indicated open connections. Therefore, metal layers have been deposited on the pads of the implant to create an interface with the purpose of easing the assembly and improving the adhesion between Au stud bumps and graphene. Initially, only Al has been used as a metal interface since it is considered a good candidate for bonding processes but it has been noticed that there is poor adhesion between it and graphene [12]. Later, a stack of Ti and Al layers has been chosen to serve as an interface since Ti has been proven to have a good contact resistance with graphene [12] but it is not considered a good material for bonding processes.

Fig. 10(a) depicts a visual representation of the structures before and after flip-chip bonding. In Fig. 10(b), a computed tomography (CT) scan, after the bonding process is illustrated and it can be seen that the bumps have a coined-like shape, indicating that contact between the dummy chip and the substrate was made. In 10(c) a 2-point measurement result is shown. The resistance, ~8.9 kΩ, is the sum of the ball-bond and 2 graphene tracks resistances.

A second attempt of bonding dummy chips directly on graphene was performed using an ACA with nickel (Ni) particles. The 2-point measurement results are presented in Fig. 11 and it can be observed that they are similar

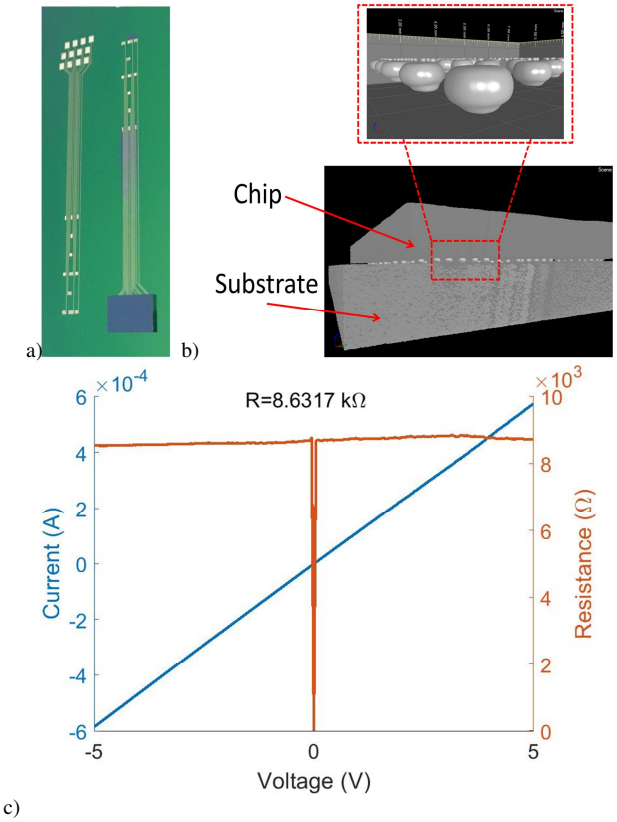


Fig. 10. Preliminary results after bonding. CT scans and 2-point measurements have been performed to ensure that the bonding process was successful.

(resistance value ~7.2 kΩ) to the previous case where a metal interface has been used for flip-chip bonding. This indicates that the Ni particles in the ACA adhere better to graphene than Au, thus creating a stable bonding interface between the stud bumps of the chip and the graphene substrate, without the need of depositing and patterning a metal layer on top of graphene. The chemistry behind this process is outside the scope of this research project.

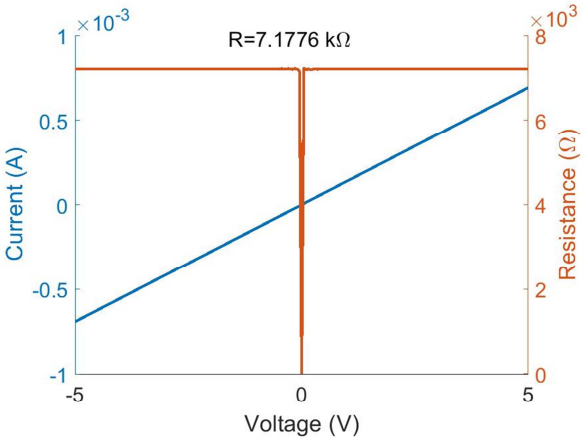


Fig. 11. 2-point measurement results for dummy chips bonded on a graphene substrate using a conductive adhesive (CA) flip-chip bonding technique.

Currently new devices are being fabricated which will allow the measurement of the flip-chip ball-bond only.

In the future, to meet the tight area requirements for the envisioned epidural monitoring implant the assembly will have to be performed with thin chips, which present unique handling challenges [13].

Moreover, before performing any *in-vivo* experiments, the implants have to be thoroughly characterized *in-vitro*. This implies optical transmittance evaluation, to establish the degree of transparency of the final device as well as electrical characterization to determine the signal to noise ratio (SNR) of graphene electrodes, important as low amplitude signals are expected to be recorded from the biological tissue. Apart from that, connecting the final device to the outside recording system constitutes a major challenge due to the small feature size of the test pads and the softness of the implant.

Once all these aspects are investigated outside the body, *in-vivo* experiments can be conducted in order to evaluate the biocompatibility of the materials used, mainly how the spinal cord reacts to graphene electrodes and PDMS encapsulation, as well as the reliability of the implant after it is implanted at its intended site, as in [14].

## IV. Conclusions

This work presents the process for developing flexible, active, graphene-based epidural spinal cord monitoring implant, by means of microfabrication only. It has been shown that F2R approach can be used to suspend large areas of the graphene-on-PDMS structures, on the Si substrate, thus avoiding as much as possible wet process steps that can cause damage to the devices. Moreover, it has been demonstrated that flip-chip bonding of chips on a graphene substrate, using either metal interfaces or conductive adhesives, is possible and initial measurements have shown that there is electrical conductivity after the bonding process. To the authors' best knowledge, this is the first work that aims to fabricate a graphene-based active implant that can be used to enable in-situ recording of the evoked activity of optically activated neuronal populations during optogenetic spinal cord stimulation.

## Acknowledgments

We acknowledge the staff of the Else Kooi Laboratory (EKL) from Delft University of Technology and Fraunhofer Institute for Reliability and Microintegration IZM for their support.

## References

[1] R. van den Brand et al., "Restoring voluntary control of locomotion after paralyzing spinal cord injury", *Science*, vol. 336, no. 6085, pp. 1182-1185, 2012.

[2] K. L. Montgomery, S. M. Iver, A. J. Christensen, K. Deisseroth, and S. L. Delp., "Beyond the brain: Optogenetic control in the spinal cord and peripheral nervous system," *Science Transl. Med.*, vol. 8, no. 337rv5, pp. 1 – 12, May 2016.

[3] V. Giagka, A. Demosthenous, and N. Donaldson, "Flexible active electrode arrays with ASICs that fit inside the rat's spinal canal," *Biomed. Microdev.*, vol. 17, no. 6, pp. 106 – 118, Dec. 2015.

[4] I. R. Minev et al., "Electronic dura mater for long-term multimodal neural interfaces", *Science,* vol. 347, no. 6218, pp 159-163.

[5] D. W. Park et al., "Graphene-based carbon layered electrode array technology for neural imaging and optogenetic applications", *Nature Communications*, vol. 5, no. 5258, pp. 1 – 11, Oct. 2014.

[6] J. Y. Hong, W, Kim, D. Choi, J. Kong, and H. S. Park, "Omnidirectionally stretchable and transparent graphene electrodes," *ACS Nano*, vol. 10, pp. 9446 – 9455, Sept. 2016.

[7] S. Vollebregt et al., "A transfer-free wafer-scale CVD graphene fabrication process for MEMS/NEMS sensors", In Proc. *IEEE MEMS*, pp.17 – 20, Sanghai, China, Jan. 2016.

[8] B. Mimoun, V. Henneken, A. van der Horst, and R. Dekker, "Flex-to-rigid (F2R): A generic platform for the fabrication and assembly of flexible sensors for minimally invasive instruments", *IEEE Sensors*, vol. 13, no. 10, pp. 3873 – 3882, Mar. 2013.

[9] Y. Wu et al.,"Synthesis of large-area graphene on molybdenum foils by chemical vapor deposition", *Carbon,* vol. 50, no. 14, pp. 5226-5231, Nov. 2012.

[10] Z. Jian et al., "Irradiation effects of graphene and thin layer graphite induced by swift heavy ions", *Chinese Physics B,* vol. 24, no. 8, June 2015.

[11] Y. Y. Wang et al., "Raman Studies of Monolayer Graphene: The Substrate Effect", *J. Phys. Chem.*, vol. 112, no. 29, pp. 10637-10640, June 2008.

[12] S. Shi, "Effects of Silicon Oxides as Substrates for Graphene-based Gas Sensor", *TU Delft*, 2017

[13] V. Giagka, N. Saeidi, A. Demosthenous, and N. Donaldson, "Controlled silicon IC thinning on individual die level for active implant integration using a purely mechanical process," in Proc. *ECTC 2014*, Orlando, FL, USA, May 2014, pp. 2213 – 2219.

[14] V. Giagka, A. Vanhoestenberghe, N. Wenger, P. Musienko, N. Donaldson, and A. Demosthenous, "Flexible platinum electrode arrays for epidural spinal cord stimulation in paralyzed rats: An in vivo and in vitro evaluation," in Proc. *3rd Annual Conf. IFESSUKI 2012*, Birmingham, UK, Apr. 2012, pp. 52 – 53.